ELSEVIER

Journal of Chromatography A, 683 (1994) 203–214

JOURNAL OF
CHROMATOGRAPHY A

Simultaneous gas chromatographic–Fourier transform infrared spectroscopic–mass spectrometric analysis of synthetic fuel derived from used tire vacuum pyrolysis oil, naphtha fraction

Hooshang Pakdel*, Christian Roy

Department of Chemical Engineering, Université Laval, Ste-Foy (Québec) G1K 7P4, Canada

Abstract

Used tires were pyrolysed in a process development unit under vacuum at about 510°C and yielded 45% oil from which 27% (w/w) of a naphtha fraction (initial boiling point, IBP: 204°C) was separated. A new gas chromatographic configuration by combining infrared, mass spectrometric and flame photometric detectors to simultaneously analyze the effluent from a single capillary column injection was tested. Over 150 compounds were identified and quantified. Sulfur compounds distribution was established by sulfur-specific detection and selected ion GC–MS. Unlike petroleum, tire-derived pyrolytic naphtha is composed of highly branched chain isomeric hydrocarbons. Infrared spectroscopy as an extremely sensitive isomer-specific probe of molecular structures is described. Over 50 compounds were positively characterized by combining MS and IR data. It is shown that mass spectrometry provides superior quantitative capabilities, while infrared spectroscopy is an excellent complementary technique for simultaneous qualitative analysis of pyrolysis oils. Some of the difficulties encountered in the present application are discussed.

1. Introduction

Each year approximately 250 millions of used tires are discarded in the USA and about 24 millions in Canada. While about 20% of the used tires are recapped, most are dumped in the rural areas, which threatens the environment. Approximately one worn tire is produced per person per year in the developed countries.

Tire is principally a vulcanized rubber compound made of styrene–butadiene (SBR) polymer with about 25% styrene. Other elastomers such as natural rubber, synthetic *cis*-polyisoprene and *cis*-polybutadiene have also been used with SBR in different proportions [1]. Typically a tire is composed of 50% rubber, 27.5% carbon black, 17.5% extender oil and 5% of other ingredients.

If recycled, used tires are a source of energy and chemicals. Many processes have been described for the pyrolysis of old tires which yield oil, carbon black and gas using different heating systems and reactor configurations [1–3]. A vacuum pyrolysis unit with a design throughput capacity of 100 kg/h is available in our laboratories. The equipment has been described elsewhere [4]. Vacuum pyrolysis has several advantages due to the short gas and vapour residence time in the reactor and rather low decomposition temperature which minimizes sec-

---

* Corresponding author.

0021-9673/94/$07.00
SSDI 0021-9673(94)00535-H

ondary reactions. In addition, the carbon black solid residue and liquid oil are recovered separately. The oil yield is also considerably increased under vacuum compared to the atmospheric pressure conditions. The pyrolysis oil obtained under vacuum contains a significant portion of a volatile, naphtha-like fraction with an octane number similar to petroleum naphtha. Pyrolysis oil may be used directly as fuel or added to petroleum refinery feedstocks. The oil may also be used as an important source of chemicals such as benzene, toluene, xylene and limonene [5]. The non-condensable gases are used as a make-up heat source for the process and the solid char may be used either as smokeless fuel, carbon black or activated carbon [6].

In order to utilize the crude pyrolysis naphtha as refining feedstock, it is necessary to obtain comprehensive data on the physical and chemical properties of the oils. The information is important in many ways: to determine if environmentally hazardous components exist in the oil; to find out whether any nitrogen and sulfur compounds exist which need to be removed or treated before catalytic upgrading; and to establish the basic composition of the oil in order to determine the products to be refined from the oil.

Previous studies have concentrated on engineering aspects of rubber pyrolysis but detailed analyses of both the pyrolysis oil and the solid products are rarely reported. This paper reports a detailed chemical analysis of the pyrolysis oil naphtha fraction.

For a number of years, gas chromatography–mass spectrometry (GC–MS) has been accepted as the method of choice for the analysis of volatile to semi-volatile compounds. However, there are some limitations to the use of the benchtop GC–MS systems. For instance, under electron impact (EI) ionization at 70 eV, these systems often do not allow the differentiation of isomers because they lack structurally specific cleavages. In order to achieve a higher level of confidence in the identification, it is necessary to use complementary techniques which indicate the position and the nature of the substitution groups. The recent development of Fourier transform infrared (FTIR) spectroscopy and more particularly its coupling with chromatography techniques (GC–FTIR) have led to its application in the field of pollutant analysis [7,8]. Very recently, product analysis data based on GC–MS and GC–FTIR techniques enabled Dubey et al. [9] to propose a degradation mechanism for butyl rubber. Though GC–FTIR is less sensitive than GC–MS, it offers the advantage of differentiating isomers. An improved chromatographic resolution by means of programmed speed deposition and higher sensitivity than light-pipe-based GC–FTIR measurement has been achieved by a GC–matrix isolation–FTIR technique [10].

One of the main difficulties in GC separation is the complexity of sample matrices such as complex hydrocarbon mixtures derived from pyrolysis of rubber which results in peak overlap and incorrect identifications. Nitrogen- and sulfur-containing compounds in rubber pyrolysis oils are in low proportion and are difficult to identify and consequently have to be fractionated prior to analysis. Krock and Wilkins [8] have developed a multidimensional GC–FTIR–MS method to analyze complex organic pollutants. They used two GC columns in series. The multicolumn analysis can be replaced by a single column with higher resolution as discussed in this paper. Due to its high and complex isomeric hydrocarbon nature, pyrolysis naphtha is a good example to test potential applications of FTIR combined with GC and MS.

2. Experimental

The pyrolysis oil sample used in this investigation was produced from used tires in a vacuum pyrolysis process development unit (PDU). The system operated on a semicontinuous feed mode using punched cross-ply tire particles. The throughput capacity was 19 kg/h. The reactor maximum temperature and total pressure were 510°C and 33 kPa, respectively. The experiment has been identified as run H04 and the system operation has been described in detail elsewhere [4]. The process yielded 45.0%

(w/w) oil, 25.0% carbon black and 30.0% gas during the run. A pyrolytic oil sample with elemental composition of typically 88.2% carbon, 8.5% hydrogen, 1.1% nitrogen, 1.2% sulfur and 1.0% oxygen was distilled under atmospheric pressure up to 204°C to separate the naphtha fraction.

GC analysis was performed on a Hewlett-Packard HP 5890 gas chromatograph equipped with a flame photometric detection (FPD) system for sulfur analysis at 280°C and a 100 m × 0.25 mm I.D. Petrocol DH capillary column from Supelco with 0.50 μm film of bonded methyl silicone and 0.45 ml/min flow-rate and nitrogen as the make-up gas. Injection mode was split at 250°C with about 1:150 split ratio. The column was directly introduced in the FPD system for GC–FPD operation or in the ion source of a Hewlett-Packard HP 5970 series mass-selective detector for GC–MS operation. Typical MS operating conditions were as follows: transfer line 270°C, ion source 250°C, electron energy 70 eV. Data acquisition was done with HP-UX Chemstation software using a Hewlett-Packard HP-UNIX computer and NBS library data base. The mass range m/z 30–400 dalton was scanned every 1.0 s. The main objective to choose a 100-m long capillary column with a thick stationary phase (0.5 μm) was to have a high resolution and loading capacity for this particular analysis of naphtha-like volatile hydrocarbon mixture. It is not however recommended for the analysis of low-volatile mixtures. Since IR is at least a hundredfold less sensitive compared with MS, a large sample volume can be injected on a 100-m column for the IR detection without overloading the column. GC–MS analysis was successfully performed by injecting 0.8 μl of pure naphtha on a 100-m column. Maximum column head pressure was 200 kPa which only produced about 0.45 ml/min column flow-rate. Due to the low flow-rate and large pressure drop across the light-pipe this flow was insufficient for GC–FTIR–MS analysis. A pressure regulator which can control about 680 kPa should replace the existing GC pressure regulator. The required modification will be made for the future analysis. The present GC–FTIR–MS results were obtained by injecting 1-μl samples on a 30 m × 0.25 mm I.D. HP5-MS fused-silica capillary column from Hewlett-Packard with 0.25 μm film thickness. The column flow-rate was 0.9 ml/min and 1:150 split ratio.

GC–FTIR–MS operation was performed on a Bio-Rad FTS45 IR detector interfaced to the same HP gas chromatograph with a split injec-

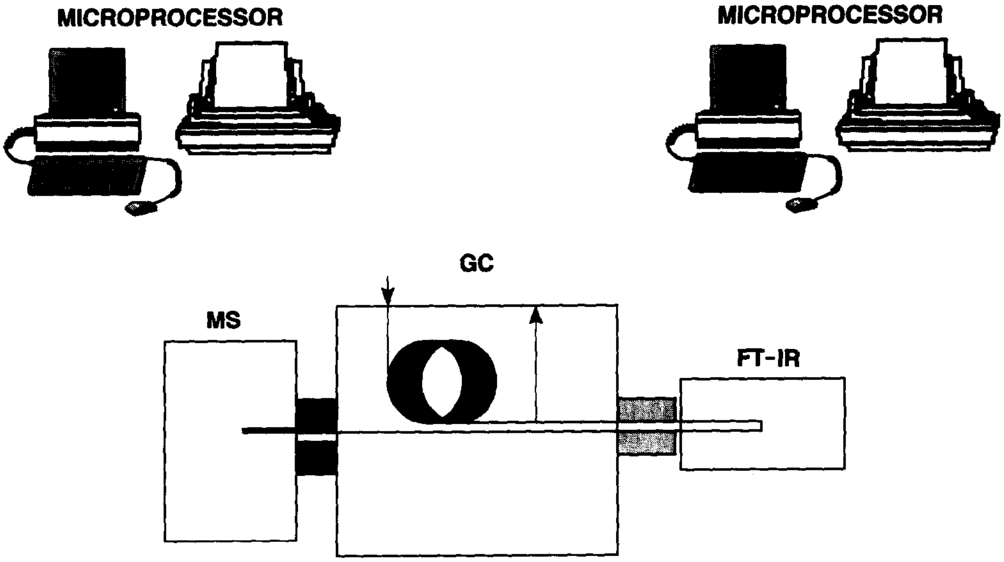

Fig. 1. Schematic diagram of simultaneous GC–FTIR–MS analyses.

tor. FTIR spectra were obtained by collecting 4 scans per scan-set using a narrow-band mercury cadmium telluride (MCT) detector with a spectral cutoff of 750 cm^{-1} and an optical resolution of 8 cm^{-1}. This corresponds to the collection of 4 spectra per second. The FTIR interface has a 10 cm × 1 mm I.D. column internally gold-coated Pyrex light pipe that was maintained at 250°C. The optics of the FTIR were purged with dried air supplied by Blaston 75-62 purge gas generator (Haverhill, MA, USA). GC oven temperature conditions were as follows:

GC–MS and GC–FPD analyses: the oven temperature was initially set at 35°C for 10 min, then programmed to 130°C at 2°C/min. Then it was programmed to 250°C at 30°C/min. It was set at 250°C for 5 min. GC–MS and GC–FPD analyses were performed separately under similar GC conditions.

GC–FTIR–MS analyses: the oven temperature was initially set at 35°C for 10 min, then programmed to 150°C at 4°C/min. Then it was programmed to 250°C at 30°C/min. It was set at 250°C for 5 min. These analyses were performed simultaneously. The experimental arrangement is shown schematically in Fig. 1. The mass-selective detector was physically located on the left side of the gas chromatograph in the standard Hewlett-Packard configuration, while the FTIR instrument was located on the right side with the front of the instrument in a reverse position to that of the gas chromatograph. Due to its short length, the light-pipe rigid-heated transfer line was temporarily modified by extending a couple of centimeters. This arrangement permitted the interface to be matched to the GC system.

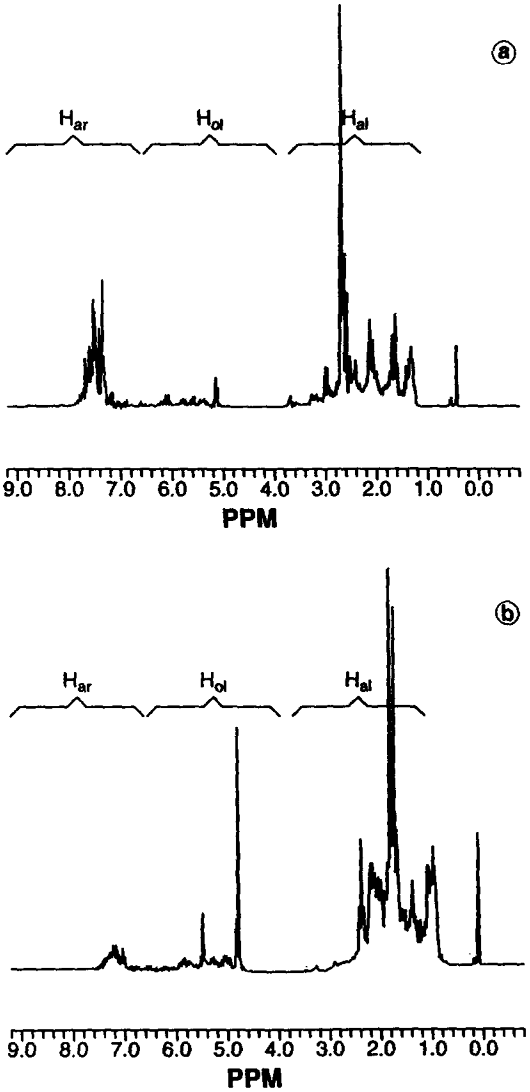

Fig. 2. 300 MHz ^{1}H FTNMR spectra of pyrolytic naphtha obtained at (a) 33 kPa pyrolysis pressure, (b) 13 kPa pyrolysis pressure.

3. Results and discussion

Pyrolysis oil composition depends on the pyrolysis conditions. Pyrolysis under high pressure yields higher content of high-volatile aromatic and lower content of olefinic compounds than low-pressure pyrolysis. Fig. 2 shows high-field proton FTNMR spectra of naphtha fractions recorded on a 300 MHz Brucker spectrometer. Naphtha in Fig. 2a was obtained under 33 kPa pyrolysis pressure while naphtha in Fig. 2b was obtained under 13 kPa (run H03). Fig. 2a represented 21.4% and 1.3% aromatic (H_{ar}) and olefinic (H_{ol}) protons, respectively. But Fig. 2b represented 2.7% H_{ar} and 9.3% H_{ol} protons, respectively. Volatile aromatic hydrocarbons have potential industrial applications such as solvent and octane booster for gasoline. However, a detailed characterization of pyrolytic

Table 1
Tentative characterization of pyrolytic naphtha by GC–MS

t_R (min)[a]	% (w/w)	Tentative assignment	t_R (min)[a]	% (w/w)	Tentative assignment
12.49	0.07	Acetonitrile	38.24	0.01	2,4-Heptadiene
14.28	0.025	1,4-Pentadiene	38.56	0.71	1,5-Dimethylcyclopentene
15.07	0.02	1,1-Dimethylcyclopropane	39.06	9.08	Toluene
15.85	0.02	2-Methyl-1-buten-3-yne	39.32	0.22	3-Methylthiophene
16.61	0.11	Propanenitrile	39.45	0.22	3-Methyl-1,3,5-hexatriene
17.14	0.005	Cyclopentene	39.56	0.12	Cyclopentanone
18.87	0.005	2-Methyl-2-propenenitrile	39.73	0.09	3-Methyl-2,4-hexadiene
20.01	0.035	1-Hexene	40.13	0.08	2-Methylthiophene
20.65	0.03	2-Methylpropanenitrile	40.31	0.35	Methylenecyclohexane
21.07	0.03	Hexane	40.45	0.33	2-Methyl-1,3,5-hexatriene
21.70	0.02	2-Methyl-2-pentene	40.64	0.32	5,5-Dimethyl-1,3-cyclopentadiene
21.96	0.02	3-Methyl-1,3-pentadiene	41.74	0.11	1,4-Dimethylcyclohexane
22.06	0.02	3,3-Dimethyl-1-butene	42.08	0.06	2,3-Dimethyl-1,4-hexadiene
22.21	0.025	2,3-Dimethyl-1,3-butadiene	42.63	0.08	2-Methyl-1-heptene
22.66	0.025	2-Methyl-1,3-pentadiene	43.09	0.32	1-Octene
23.04	0.10	3-Methyl-2-pentene	43.44	0.19	1,3,5-Heptatriene
24.14	0.01	4-Methyl-2-pentene	43.64	0.52	2-Methylpyridine
24.28	0.09	2-Methyl-1,3-pentadiene	44.45	0.10	3-Methylcyclohexanone
24.52	0.19	1,3-Cyclohexadiene	44.66	0.12	1,4-Dimethylcyclohexane
24.64	0.09	1,1-Dimethyl-2-methylenecyclopropane	45.12	0.07	3-Ethyl-1,4-hexadiene
24.92	0.25	1,3,5-Hexatriene	45.34	0.24	2,3,3-Trimethyl-1,4-pentadiene
25.38	0.05	2,4-Hexadiene	45.34	0.01	5-Methyl-1,3,6-Heptatriene
25.98	0.07	1,4-Hexadiene	45.95	0.19	2-Methyl-1H-pyrrole
26.06	0.06	1,1-Dimethyl-2-methylenecyclopropane	45.16	0.11	Cyclohexanone
26.17	0.14	1-Methylcyclopentene	46.90	0.38	2,3,3-Trimethyl-1,4-pentadiene
26.29	1.21	Benzene	47.07	0.21	2,3-Dimethyl-1,4-hexadiene
26.84	0.04	4,4-Dimethyl-2-pentene	47.37	0.30	3-Methyl-1,4-heptadiene
27.67	0.16	5-Methyl-1,3-cyclopentadiene	47.71	0.24	4-Ethenylcyclohexene
29.13	0.09	Bicyclo[3.1.0]hexane	47.90	0.07	Ethenylcyclohexane
30.88	0.12	1-Heptene	47.94	0.08	1-Ethenylcyclohexene
31.83	0.04	2-Heptyne	48.30	0.04	2,3-Dimethyl-2-hexene
32.13	0.16	4-Methyl-1,4-hexadiene	48.53	0.13	1-Ethylcyclohexene
32.32	0.08	1,5-Dimethylcyclopentene	48.66	0.46	3-Methylpyridine
32.53	0.07	2-Methyl-2-hexene	49.02	0.23	3-Ethylidene-1-methylcyclopentene
32.85	0.035	1-Heptene	49.27	0.06	Bicyclo[5.1.0]octane
32.23	0.06	2-Methylenebutanenitrile	49.64	1.58	Hexanenitrile
33.42	0.06	3-Methyl-2-hexene	49.86	0.13	1-Ethylcyclohexene
33.57	0.10	4,4-Dimethylcyclopentene	50.29	3.21	Ethylbenzene
34.08	0.06	4-Methyl-2-hexyne	50.46	0.20	3-Ethylthiophene
34.44	n.a.	3-Ethylcyclopentene	50.93	0.12	2,3-Dimethyl-1,4-hexadiene
34.73	0.04	Pyridine	51.05	n.a.	2,5-Dimethylthiophene
34.84	0.17	3-Methyl-1,3,5-hexatriene	51.39	13.46	*m*-Xylene
35.30	0.13	Pentenenitrile	51.65	0.24	Tetramethylmethylenecyclopropane
35.68	0.11	2,3,4-Trimethyl-2-pentene	51.75	0.12	2,3-Dimethylpyridine
35.78	0.02	2,3-Dimethyl-1,4-hexadiene	51.90	0.10	2,4-Dimethylthiophene
36.28	0.48	1H-Pyrrole	52.35	0.31	Trimethyl-1,3-cyclopentadiene
36.51	0.34	3-Methyl-1,3,5-hexatriene	52.60	0.07	1,2-Dimethylcyclohexene
36.64	0.16	4-Methylcyclohexene	52.92	0.13	Ethenylthiophene
36.87	0.13	1-Methyl-1,4-cyclohexadiene	53.05	0.17	2,3-Dimethylthiophene
37.23	0.76	Nitrile derivative	53.26	2.59	1,3,5,7-Cyclooctatetraene
37.53	0.16	1,2-Dimethyl-1,3-cyclopentadiene	53.60	0.18	3-Octen-1-yne

(Continued on p. 208)

Table 1 *(continued)*

t_R (min)[a]	% (w/w)	Tentative assignment
53.68	0.10	Trimethylcyclopentadiene
53.85	3.93	*p*-Xylene
54.15	0.23	2-Methylene-4-pentenenitrile
54.45	0.01	1-Methylene-3-(1-methylethylidene)-cyclopentane
54.55	0.62	1-Nonene
55.23	0.24	Trimethyl-1,3-cyclopentadiene
55.78	0.19	Nonane
56.03	0.15	Trimethyl-1,3-cyclopentadiene
57.14	0.01	3,5-Octadiene-2-ol
57.31	0.56	Isopropylbenzene
57.41	0.01	1,2,6,6-Tetramethyl-1,3-cyclohexadiene
57.77	0.08	1-Methyl-3-(1-methylethylidene)-cyclopentane
58.81	0.39	α-Ethylbenzenemethanol
59.26	0.34	1-Ethenyl-2-methylbenzene
60.23	0.34	2,5-Dimethyl-3-methylene-1,5-heptadiene
60.40	0.56	Benzeneacetaldehyde
60.91	0.48	Aniline
60.91	n.a.	2-Isopropylthiophene
61.16	3.27	*o*-Ethyltoluene
61.42	1.71	*m*-Ethyltoluene
61.93	1.11	1,3,5-Trimethylbenzene
62.48	0.20	1,4-Dimethyl-5-isopropylcyclopentene
62.86	0.77	Isopropenylbenzene
62.99	0.77	*p*-Ethyltoluene
63.18	0.12	2,3,4-Trimethylthiophene
63.90	0.14	Propenylbenzene
64.20	1.05	α-Ethenyltoluene
64.35	0.18	Cyclopropylbenzene
64.49	3.60	1,2,4-Trimethylbenzene
64.79	0.49	1-Ethyl-2-pentylcyclopropane
65.41	0.55	1,2,3,4,5-Pentamethyl-1,3-cyclopentadiene
65.53	0.10	4,5-Dimethyl-2,6-octadiene
65.87	0.19	Decane
66.11	0.01	2,5,6-Trimethyl-1,3,6-heptatriene
66.55	0.19	1,5-Dimethyl-6-methylene-spiro[2.4]-heptane
66.72	0.01	2,5-Diethylthiophene
67.23	1.71	1,2,3-Trimethylbenzene
67.51	0.81	Tetramethylbenzene
68.10	0.20	4-Isopropyl-1-methylcyclohexene
68.43	2.54	*dl*-Limonene
68.76	0.04	*o*-Isopropyltoluene
69.01	0.90	1-Propenylbenzene
69.31	0.10	Camphene
69.54	0.22	1-Methyl-2-pentylcyclohexane
69.71	0.16	1,2,3,5-Tetramethylbenzene
69.97	0.23	*m*-Propyltoluene
70.32	0.18	Diethylbenzene
70.54	0.72	1,4-Dimethyl-2-ethylbenzene
71.47	0.12	*p*-Propyltoluene
72.32	0.13	3,5-Dimethyl-1-ethylbenzene
72.53	0.48	*m*-Isopropyltoluene
72.74	0.13	2,3-Dihydro-5-methyl-1H-indene
73.06	0.19	3,5-Dimethyl-1-ethylbenzene
73.21	0.52	2-Butenylbenzene
73.72	0.16	1,2-Dimethyl-4-ethenylbenzene
74.06	0.23	2-Undecene
74.31	0.09	1,3-Dimethyl-2-ethenylbenzene
74.65	0.08	*p*-Isobutyltoluene
74.03	0.14	Undecane
75.67	0.02	2,3-Dihydro-1,6-dimethyl-1H-indene
76.03	0.10	1,2,3,5-Tetramethylbenzene
76.33	0.40	1,2,3,5-Tetramethylbenzene
76.65	0.02	2-Ethenyl-1,3,5-trimethylbenzene
76.75	0.08	*o*-Propenyltoluene
76.98	0.01	1,3-Dimethyl-2-ethenylbenzene
77.94	0.12	2,3-Dihydro-5-methyl-1H-indene
78.87	0.11	2,3-Dihydro-4-methyl-1H-indene
79.11	0.26	1-Methyl-1H-indene
79.27	0.07	1-Butynylbenzene
79.40	0.01	2-Methylbutylbenzene
79.83	0.07	1,2,3,4-Tetrahydronaphthalene
79.95	0.01	1,3-Butadienylbenzene
80.97	0.01	(2-Methyl-1-butenyl)benzene
80.31	0.01	1,2-Dihydro-2-methylnaphthalene
81.56	0.12	Naphthalene
82.03	0.02	2,3-Dihydro-1,2-dimethyl-1H-indene
82.52	0.05	2-Decene
82.94	0.02	2,3-Dihydro-1,3-dimethyl-1H-indene
83.96	0.01	Benzothiazole
85.27	0.07	3,5-Dimethyl-1-ethyl-1H-pyrazole
87.49	0.08	1,1-Dimethyl-1H-indene
87.98	0.01	1,2-Dihydro-2-methylnaphthalene
88.70	0.01	1,2-Dihydro-3-methylnaphthalene
90.61	0.025	1-Methylnaphthalene
Total	80.19	

n.a. = Not available.

[a] Retention time, see Fig. 3.

naphtha fraction is prerequisite for its application. Vacuum pyrolysis of used tires typically yields 20–28% (w/w) of naphtha fraction.

Table 1 shows an extended list of compounds that were tentatively identified by GC–MS on a 100-m column. The compounds listed are esti-

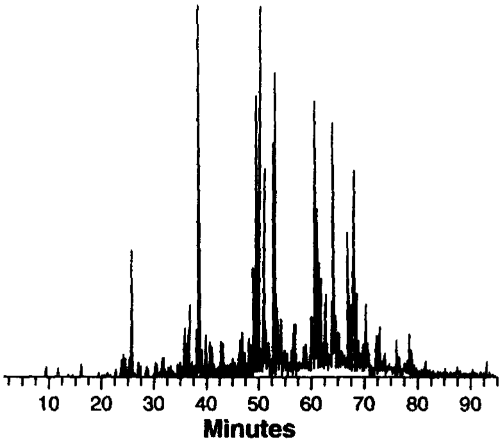

Fig. 3. Total ion chromatogram of pyrolytic naphtha.

mated to be over 80% of the total naphtha composition. Some of the results are not yet fully confirmed by GC–FTIR–MS. The total ion chromatogram is shown in Fig. 3. This chromatogram was recorded by injecting 0.8 μl of the pure sample without significantly affecting the column resolution. The sample was found extremely complex. Nevertheless, a satisfactory resolution was achieved which has motivated future GC–FTIR–MS analysis on the same column after modification of the GC flow supplier. Due to the large number of isomeric compounds (Table 1), in many cases MS failed to make unambiguous isomer-specific identification. However, Table 1 lists only the most probable isomeric structures identified by MS search file system. In close agreement with Fig. 2, Table 1 shows that the majority of compounds are substituted aromatic hydrocarbons with various isomers. Benzene, toluene, xylene, trimethylbenzene and tetramethylbenzene are the most abundant aromatic components of tire pyrolysis-derived naphtha fraction. The relative mass percentages of the individual compounds were calculated by assuming the same response factor from the peak areas of the chromatogram shown in Fig. 3. Results are presented in Table 1. Most of the volatile aliphatic and alicyclic hydrocarbons have similar GC responses near unity. Linear hydrocarbons are mainly concentrated in the first 25 min of the chromatogram (m/z 41 is the characteristic fragment ion peak) followed by benzene (m/z 78), mono-, di-, tri- and tetra-substituted benzenes (m/z 92, 91, 105 and 119, respectively) and finally indene (m/z 116) and naphthalene (m/z 128) derivatives. Substituted benzene derivatives appeared in decreasing order of abundance from mono- to tetra-substituted benzene and are depicted in selected ion chromatograms (m/z 91–119) shown in Fig. 4.

dl-Limonene is one of the most important constituents of pyrolytic naphtha with potential economic value [5]. Its concentration drastically decreased as the reactor pressure increased. Approximately 25% *dl*-limonene has been reported by this laboratory earlier under about 2.7 kPa total pressure [5]. Atmospheric pressure pyrolysis yielded practically no *dl*-limonene [11]. Moreover, the substantial proportion of monoaromatic hydrocarbons present in the naphtha fraction suggests that this oil could become a potential feedstock for the production of aromatic solvent and BTX (benzene, toluene and xylene) or a high-octane gasoline pool (a blend of various gasolines).

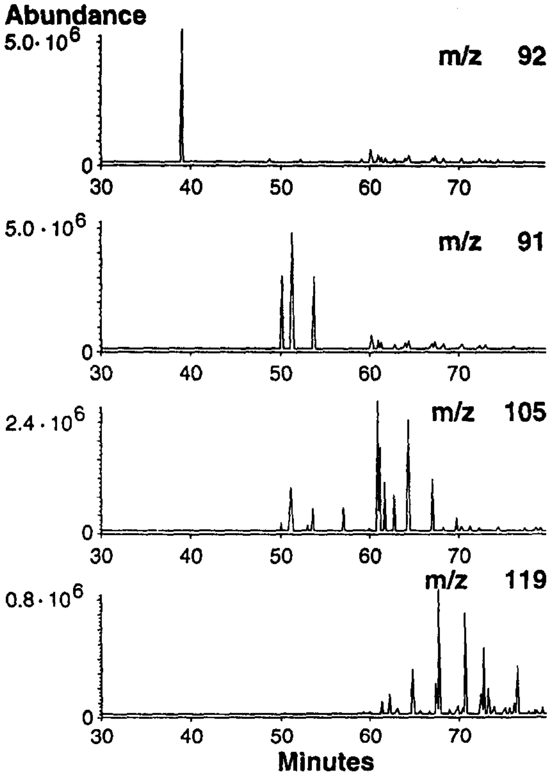

Fig. 4. Ion chromatograms of pyrolytic naphtha.

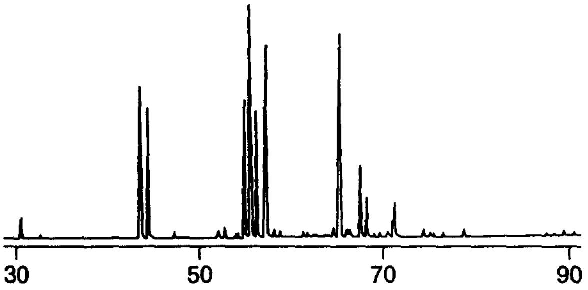

Fig. 5. Gas chromatogram of sulfur compounds in pyrolytic naphtha.

Table 2
Sulfur compounds identified in pyrolytic naphtha

Peak No.[a]	Assignment
1	2-Methylthiophene
2	3-Methylthiophene
3	2-Ethylthiophene
4	2,5-Dimethylthiophene
5	2,4-Dimethylthiophene
6	3-Ethylthiophene
7	2,3-Dimethylthiophene
8	2-Isopropylthiophene
9	2-*tert.*-Butylthiophene
10	Benzothiazole

[a] See Fig. 6.

The chromatogram in Fig. 5 was recorded on the same column and conditions as Fig. 3 using sulfur-specific FPD. Fig. 6 illustrates a reconstructed selected ion chromatograms of *m/z* 97 for $(C_5H_5S)^+$, 111 for $(C_6H_7S)^+$, 125 for $(C_7H_9S)^+$ and 135 for $(C_7H_5SN)^+$ which is in good agreement with Fig. 5. Those ions are the characteristic fragment ions (or molecular ions) of methyl-, dimethyl- and ethylthiophene; trimethyl- and isopropylthiophene; *tert.*-butylthiophene and benzothiazole, respectively. Ten major peaks of Fig. 6 were identified and are listed in Table 2. GC analysis using sulfur-specific detection helped to confirm the assignments in Table 1. Those compounds are the principal pyrolysis sulfur products derived from the vulcanization agents which have been added during the tire manufacture.

Capillary column gas chromatograms of the same oil obtained simultaneously with both IR and MS techniques are shown in Fig. 7a and b,

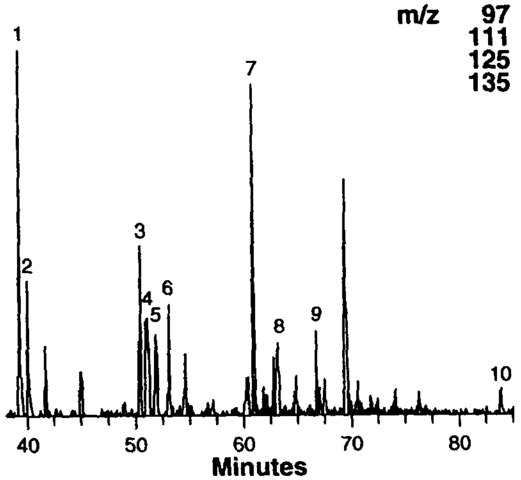

Fig. 6. Reconstructed ion chromatogram of sulfur compounds in pyrolytic naphtha.

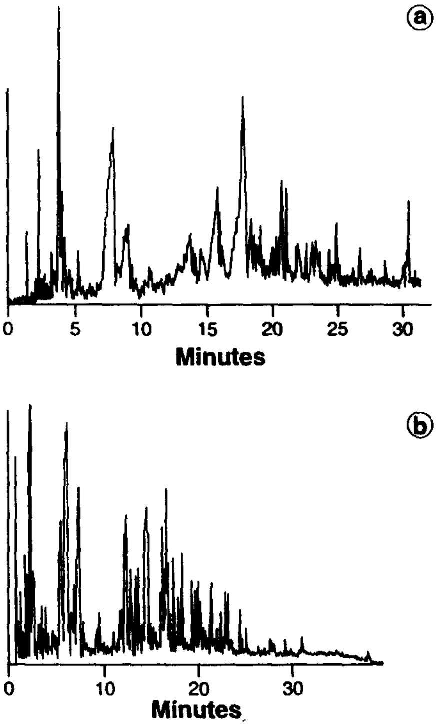

Fig. 7. Chromatograms of pyrolytic naphtha. (a) GC–FT-IR Gram–Schmidt chromatogram; (b) GC–MS total ion chromatogram.

respectively. The total ion chromatogram (Fig. 7b) was rather overloaded due to a low column loading capacity for the quantity of solution injected. The IR chromatogram in Fig. 7a shows a lower resolution compared with Fig. 7b. The chromatographic resolution can be increased if two scans are collected per scan-set at 4 cm^{-1} spectrometer resolution. Only four scans were collected at 8 cm^{-1} spectrometer resolution in this work. This experimental condition will double the file size without sacrificing the signal to noise ratio. However, most of the principal chromatographic peaks were positively identified and listed in Table 3. This example clearly illustrates the powerful and complementary nature of combined instruments. In many cases throughout the analysis where MS failed to make isomer-specific identifications, the FTIR spectra provided a positive identification of the correct compounds. However, the molecular masses from the mass spectra were equally important to establish the molecular tentative structures. MS with GC retention data or FTIR spectra alone can be used to tentatively identify many of the compounds listed in Table 1, but with far less ease and confidence than with the combined GC, MS and FTIR.

Di-, tri- and tetra-substituted benzene and ethylbenzene are the best examples which usually show quite similar isomeric mass spectra that are difficult to differentiate. These compounds are high abundant components of naphtha which have a unique IR spectra. This ability is based on specific vibrational modes associated with individual substitution patterns. The EI mass spectra of all substituted benzenes have two M$^+$ and M$^+ - 15$ ions as the base peaks. Therefore, usually all isomeric compounds show a similar mass spectra. FTIR on the other hand is very powerful to differentiate the isomeric structures. Figs. 8–10 illustrate MS and FTIR spectra of four pairs of typical benzene derivatives in pyrolytic naphtha. The isomeric pairs in Figs. 8a and b to 10a and b exhibit similar characteristic ions in their mass spectra which are impossible to be differentiated. On the other hand, FTIR spectra of these compounds reveal significant differences. These differences are based on ap-

Table 3
List of compounds identified by GC–FTIR–MS

t_R (min)[a]	Assignment
2.22	2-Methyl-1,5-hexadiene
2.35	Benzene
2.40	1,3-Cyclohexadiene
2.49	2-Methyl-1,4-pentadiene
2.56	1-Heptane
2.69	5-Methyl-1,4-hexadiene
3.24	1-Methylcyclohexadiene
3.47	1H-Pyrrole
3.50	1,2-Dimethyl-1,3-cyclopentadiene
3.77	Toluene
3.87	1,3,5-Heptatriene
4.09	2-Pentenenitrile
4.19	3-Octene (*trans*)
4.80	2-Methylpyridine
5.15	2,3-Dimethyl-1,4-hexadiene
6.61	Ethylbenzene
7.25	*m*-Xylene
8.25	Ethenylbenzene
8.36	*o*-Xylene
12.21	Propylbenzene
12.90	*m*-Ethyltoluene
13.35	1,3,5-Trimethylbenzene
13.94	*o*-Ethyltoluene
14.16	1-Methylethenylbenzene
14.92	1,2,4-Trimethylbenzene
15.15	2-Propenylbenzene
16.50	1,2,3-Trimethylbenzene
16.71	1,2,3,4-Tetramethylbenzene
16.98	*dl*-Limonene
17.15	1-Propenylbenzene
17.60	Indene
18.07	1-Methylpropylbenzene
18.28	Butylbenzene
18.49	3,5-Dimethyl-1-ethylbenzene
18.79	(1-Methylpropyl)benzene
18.87	3-Methylbenzonitrile
19.05	4-Methylbenzene
19.19	2,5-Diethylthiophene
19.32	1-Methyl-4-isopropylbenzene
19.45	1,2-Dimethyl-4-ethylbenzene
19.68	1-Methyl-1-propenylbenzene
19.75	*tert.*-Butylbenzene
20.00	2-Methylpropenylbenzene
20.19	1-Undecene
21.39	1,2,3,5-Tetramethylbenzene
22.15	2,3-Dihydro-5-methyl-1H-indene
22.62	3-Methyl-1H-indene
22.88	1-Methyl-1H-indene
23.07	Pentylbenzene
24.03	Naphthalene
24.28	2,3-Dihydro-1-dimethyl-1H-indene
24.60	1-Dodecene
25.71	Benzothiazole
27.15	1,1-Dimethyl-1H-indene
28.41	2-Methylnaphthalene
29.04	1-Methylnaphthalene

[a] Retention time, see Fig. 7.

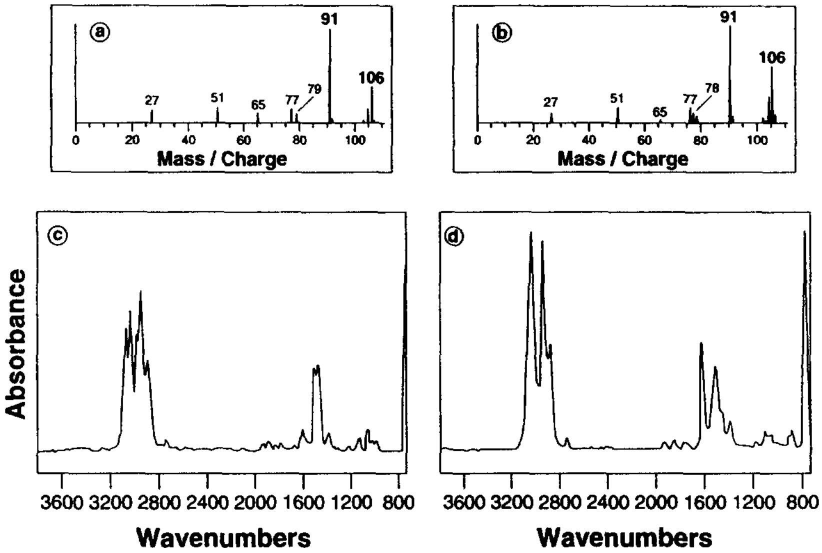

Fig. 8. MS and IR spectra of: (a, c) *o*-xylene and (b, d) *m*-xylene.

pearance or disappearance of characteristic bands or a shift to lower or higher wavelengths. Recently Smyrl et al. [12] used a single GC injection onto two capillary columns and both IR and MS analyses were performed on the separate effluents. Usually it will be very difficult to obtain similar retention time profiles in both chromatograms. The IR section requires a flow restrictor since the MS retention data will be slightly lower than IR and the spectra matching will be difficult. Interestingly, negligible retention differences were observed in this work using a single column sample injection method.

GC–FTIR–FPD was successfully tested for a standard mixture of sulfur compounds. Both MS and FTIR chromatograms showed a satisfactory

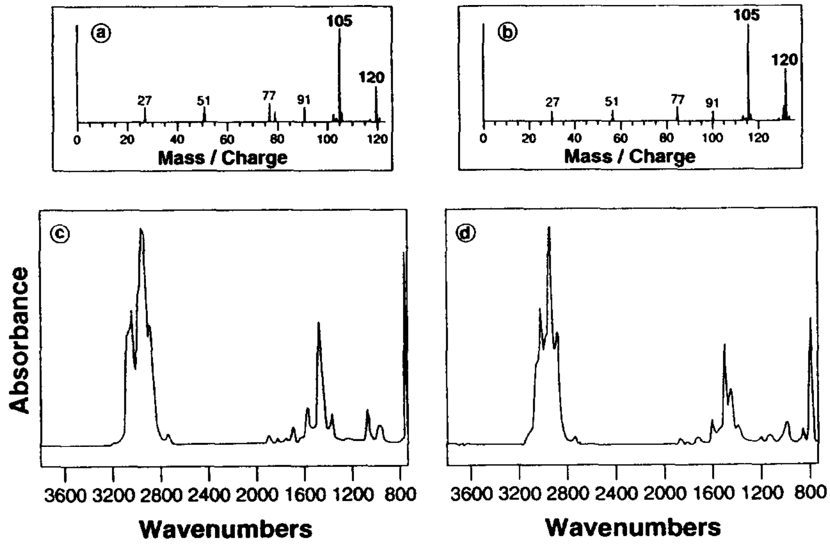

Fig. 9. MS and IR spectra of: (a, c) 1,2,3-trimethylbenzene and (b, d) 1,2,4-trimethylbenzene.

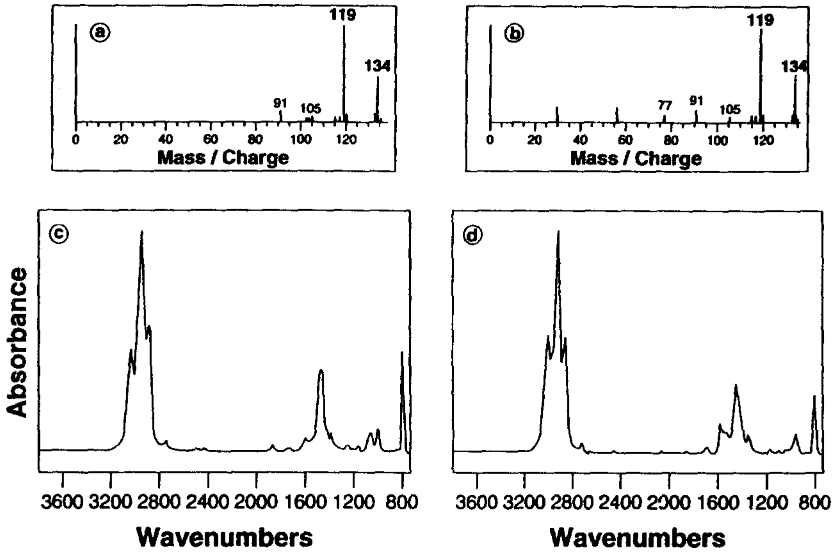

Fig. 10. MS and IR spectra of: (a, c) 1,2,3,4-tetramethylbenzene and (b, d) 1,2,3,5-tetramethybenzene.

matching retention time profile. Due to the low abundance and low GC resolution, the naphtha sulfur compounds which are listed in Table 2 could not be detected by FTIR.

Thus, it can be postulated that the higher aromatic content of the naphtha fraction analysed is associated with a relatively higher reactor pressure compared with the previous reactor configuration and conditions used [13]. However, oil composition reflects the reaction environment. It is therefore expected that a reactor can be designed and operated for specific product composition.

4. Conclusions

Used tires, when pyrolysed under vacuum, decompose to yield a complex mixture of hydrocarbon oil when analysed by GC. At 510°C and 33 kPa pressure, substituted monoaromatic hydrocarbons and their isomers were abundant in the naphtha fraction which complicated its characterization. This study has shown that a single GC injection onto a long capillary column with high loading capacity (0.5 μm stationary film thickness) and a flow-rate of about 1 ml/min enables to perform a simultaneous FTIR and MS analyses of GC effluents with matching retention times. GC–MS or GC–FTIR alone were unable for unambiguous characterization of the pyrolytic naphtha components. GC–FTIR appears, however, to be a complementary technique to GC–MS in terms of identification. Separate GC–MS and GC–FPD analyses enabled the characterization of major sulfur compounds.

References

[1] J. Dodds, W.F. Domenico, D.R. Evans, L.W. Fish, P.L. Lassahn and W.J. Toth, *Scrap Tires: A Resource and Technology Evaluation of Tire Pyrolysis and other Selected Alternate Technologies; N.T.I.S. Report No. EGG-2241*, EG & G Idaho Inc., Idaho Falls, ID, 1983.

[2] G. Crane, R.A. Elefrizt, E.L. Kay and J.R. Laman, *Rubber Chem. Technol.*, 51 (1978) 577.

[3] H. Aubin, *M.Sc. Thesis*, Université Laval, Ste-Foy (Quebec), 1987.

[4] C. Roy, B. de Caumia, D. Blanchette, H. Pakdel, G. Couture and A.E. Schwerdtfeger, *Remediation*, submitted for publication.

[5] H. Pakdel, C. Roy, H. Aubin, G. Jean and S. Coulombe, *Environ. Sci. Technol.*, 25 (1991) 1646.

[6] C. Roy, B. Labrecque and B. de Caumia, *Resour. Conserv. Recycl.*, 4 (1990) 203.

[7] H. Budzinski, Y. Hermanage, C. Pierard, P. Garrigues and J. Bellocq, *Analusis*, 20 (1992) 155.

[8] K.A. Krock and C.L. Wilkins, *Anal. Chim. Acta*, 277 (1993) 381.

[9] V. Dubey, R.K. Shrivastava, D.N. Tripathi, R.P. Semwal, B.R. Gandhe and R. Vaidyanathaswamy, *J. Anal. Appl. Pyrol.*, 27 (1993) 207.

[10] C. Klawun, T.A. Sasaki, C.L. Wilkins, D. Carter, G. Dent, P. Jackson and J. Chalmers, *Appl. Spectrosc.*, 47 (1993) 957.

[11] P.T. Williams, S. Besler and D.T. Taylor, *Fuel*, 69 (1990) 1474.

[12] N.R. Smyrl, D.M. Hembree, Jr., W.E. Davis, D.M. Williams and J.C. Vance, *Appl. Spectrosc.*, 46 (1992) 277.

[13] S. Mirmiran, H. Pakdel and C. Roy, *J. Anal. Appl. Pyrol.*, 22 (1992) 205.